Properties of magnetosheath mirror modes observed by Cluster and their response to changes in plasma parameters

Jan Soucek,[1,2] Elizabeth Lucek,[1] and Iannis Dandouras[3]

Received 17 July 2007; revised 29 October 2007; accepted 11 January 2008; published 3 April 2008.

[1] Mirror modes are large amplitude nonpropagating compressive structures frequently observed in the magnetosheath. They appear in the form of quasi-sinusoidal oscillations in the magnetic field, profound magnetic decreases (dips) or magnetic enhancements (peaks), accompanied by a corresponding anticorrelated signature in plasma density. In this study we present an analysis of the properties of mirror mode structures in the magnetosheath of the Earth based on a database of Cluster observations and also a detailed case study of one magnetosheath traversal. We focused primarily on the identification of conditions associated with the magnetic dips and magnetic peaks. It is shown that the character of mirror structures is related to the local degree of instability of the plasma with respect to the mirror instability threshold: peaks are typically observed in an unstable plasma, while mirror structures observed deep within the stable region appear almost exclusively as dips. This observation is found to be consistent with recent theoretical and numerical studies. An abrupt transition of mirror structures from peaks to dips at an approximate distance of 2 Earth radii from the magnetopause was identified by multispacecraft analysis and we interpret this effect as a consequence of plasma expansion in the vicinity of the magnetopause locally changing the plasma conditions towards a more stable state.

Citation: Soucek, J., E. Lucek, and I. Dandouras (2008), Properties of magnetosheath mirror modes observed by Cluster and their response to changes in plasma parameters, *J. Geophys. Res.*, *113*, A04203, doi:10.1029/2007JA012649.

1. Introduction

[2] Planetary magnetosheaths are regions of space filled with plasma of solar wind origin decelerated and compressed by the bow shock traversal. Conditions of moderate ion temperature anisotropy $T_\perp/T_\parallel \sim 1.2-2$ and relatively high ion beta $\beta_\parallel = 2\mu_0 nkT_\parallel/|B|^2 > 1$, characteristic for this region, are favorable for excitation of large amplitude low frequency waves (see *Schwartz et al.* [1996] for a review). Here and in the rest of the article, subscripts $\parallel$ and $\perp$ correspond to *B*-parallel and perpendicular components respectively, *n* denotes plasma ion density and *B* is the magnetic field vector.

[3] The two most important instabilities associated with an ion temperature anisotropy of type $T_\perp > T_\parallel$ are the proton cyclotron instability, responsible for excitation of transverse left-hand polarized waves, and the mirror instability that gives rise to compressional linearly polarized waves characterized by zero frequency in the plasma frame and anti-correlation of plasma density and magnetic field strength. According to the linear Vlasov theory for bi-maxwellian proton-electron plasma [*Gary*, 1992], the ion cyclotron instability grows faster for low beta plasma ($\beta_\parallel <\sim 6$), while for high beta plasmas, the mirror instability dominates. The intersection point $\beta_\parallel \sim 6$ is however strongly dependent on the relative density of Helium ions in the plasma. As shown by *Gary et al.* [1993], for moderate Helium density ($n_{He} \sim 0.03\ n_p$) typical for magnetosheath plasma, the ion cyclotron instability growth rate is reduced and the mirror instability dominates for $\beta_\parallel > \sim 1$. This latter threshold value of beta required for the growth of mirror instability is consistent with magnetosheath observations [*Anderson et al.*, 1994].

[4] The threshold value of the anisotropy required for the mirror instability to develop, derived by *Hasegawa* [1969] in cold electron bi-Maxwellian fluid approximation is given by

$$\frac{T_\perp}{T_\parallel} > 1 + 1/\beta_\perp. \tag{1}$$

Although the fluid approach is known to be insufficient to describe the physics of mirror instability and kinetic treatment is required to calculate its growth rate [*Southwood and Kivelson*, 1993; *Génot et al.*, 2001], the expression (1) still represents a correct threshold condition in the kinetic cold electron limit. This threshold condition is modified when considering nonzero temperature of electrons and electron anisotropy [*Pantellini and Schwartz*, 1995; *Stix*, 1962], but in this study we disregard these effects assuming $T_{\perp e} \approx T_{\parallel e} \ll T_\parallel$. This may result in underestimating the

[1]Space and Atmospheric Physics Group, Blackett Laboratory, Imperial College, London, UK.
[2]Department of Space Physics, Institute of Atmospheric Physics, Academy of Sciences of the Czech Republic, Prague, Czech Republic.
[3]CESR-CNRS, Toulouse, France.

0148-0227/08/2007JA012649

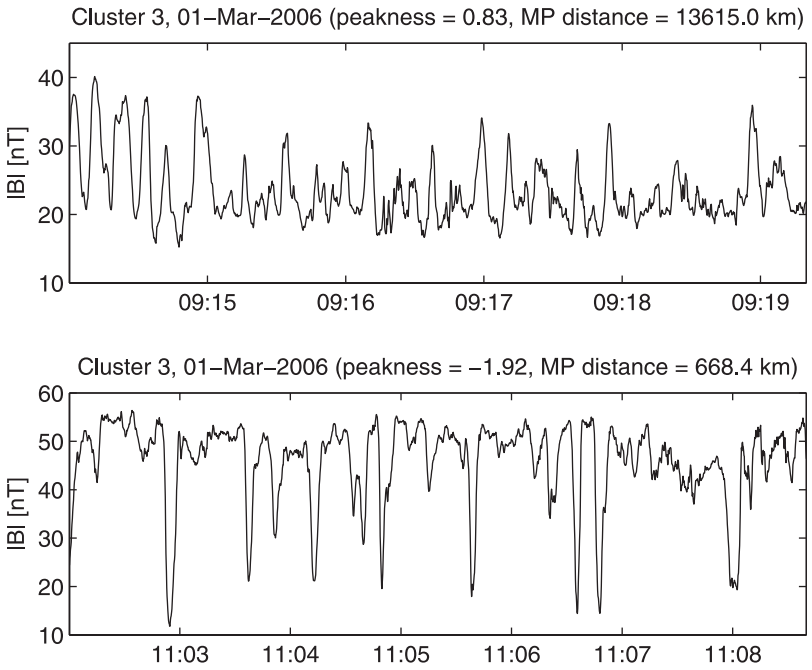

Figure 1. An example of mirror mode structures of the two types. (top) Peaks (peakness = 0.83), (bottom) dips (peakness = −1.92).

right side of inequality (1), but using the statistics of magnetosheath electron beta and anisotropy published in *Gary et al.* [2005] we estimate that this error should not exceed 10% for typical values of ion anisotropy.

1.1. Role and Evolution of Mirror Modes in the Magnetosheath

[5] Mirror mode waves (or more precisely structures) are often observed in the magnetosheath of the Earth (*Kaufmann et al.* [1970], *Tsurutani et al.* [1982] and a number of later studies), other magnetized planets [*Tsurutani et al.*, 1982; *Erdős and Balogh*, 1996; *Bavassano-Cattaneo et al.*, 1998] and recently also by Voyager spacecraft in the heliosheath [*Burlaga et al.*, 2006]. They represent a characteristic feature of high beta magnetosheath plasma; *Lucek et al.* [1999] observed mirror modes in approximately 30% of magnetosheath passes throughout the whole magnetosheath under a variety of upstream solar wind conditions. Satellite observations have confirmed that the mirror and ion cyclotron instabilities impose an upper limit on the temperature anisotropy in the magnetosheath by virtue of condition (1) and analogous threshold condition for the ion cyclotron instability [*Fuselier et al.*, 1994; *Anderson et al.*, 1994] and therefore contribute significantly to magnetosheath dynamics. A direct consequence of this β-dependent anisotropy constraint is the remarkable anti-correlation of $T_\perp/T_\parallel$ and β in magnetosheath data, suggesting that magnetosheath plasma is typically found in a marginally stable state, where the growth rate of the respective instabilities is close to zero. In their original study, *Fuselier et al.* [1994] fitted a general relation of the form

$$\frac{T_\perp}{T_\parallel} = 1 + \frac{a}{\beta_\parallel^b} \tag{2}$$

to ISEE data to obtain coefficients $a = 0.83$ and $b = 0.58$ for $\beta_\parallel > 1$. Numerous theoretical and experimental studies were later dedicated to investigating the exact form of the marginal stability relation under various conditions [*Gary et al.*, 1994; *McKean et al.*, 1994; *Samsonov et al.*, 2001]. Notably, *Hellinger et al.* [2003] and *Trávníček et al.* [2007] used hybrid simulations to study the effect of plasma compression and expansion on the mirror and ion cyclotron instabilities. They showed that if external forcing in the form of adiabatic compression or expansion is applied to the plasma, ion cyclotron and mirror instabilities respond to changes in β by correcting the temperature anisotropy and keeping the plasma in a marginally stable state.

[6] Mirror modes are typically observed not as quasi-sinusoidal waves but as trains of nonperiodic large amplitude structures of two types: local enhancements of magnetic field intensity accompanied by a simultaneous depression in plasma density (referred to as magnetic "peaks") and opposite structures, magnetic "dips", identified by a magnetic field decrease and an increase in plasma density. Examples of these two types of mirror modes are given in Figure 1.

[7] Satellite observations have shown that mirror modes are, to first order, cylindrical structures elongated in a direction approximately along the background magnetic field. They do not propagate in the plasma rest frame and are convected with the plasma flow [*Horbury et al.*, 2004; *Walker et al.*, 2002; *Constantinescu et al.*, 2003]. They are believed to represent an evolved nonlinear stage of mirror instability [*Kivelson and Southwood*, 1996], although in the case of dips, this traditional view has been questioned by the model of *Kuznetsov et al.* [2007]. Furthermore, the questions of the temporal evolution of mirror structures on the path from the bow shock to the magnetopause, their stability and the origin of the two different forms of mirror structures (peaks and dips) remain controversial to this day.

[8] Surprisingly, most experimental studies of the distribution and evolution of different types mirror structures in the magnetosheath are based on limited in-situ data from Jupiter and Saturn. *Erdős and Balogh* [1996] performed a detailed statistical study of mirror waves observed by Ulysses during a Jupiter fly-by. In their data set, mirror fluctuations were present throughout the entire magnetosheath pass and had a form of clear magnetic dips with the exception of a short interval close to the bow shock crossing. Later, a qualitative empirical model of mirror mode evolution in the magnetosheath was proposed by *Bavassano-Cattaneo et al.* [1998], based on data from the magnetosheath of Saturn, and later confirmed and extended by *Joy et al.* [2006] using Jupiter data. These studies suggested that mirror modes are generated close to the bow shock and in this early stage of development they appear as quasi-sinusoidal waves. Further downstream in the magnetosheath they approach nonlinear saturation [*Kivelson and Southwood*, 1996] and change into nonperiodic large amplitude structures of either type; both peaks and dips are observed in the middle magnetosheath. As the mirror modes are convected towards the magnetopause, notably in the plasma depletion layer, plasma becomes mirror-stable and mirror structures start to collapse and decay away. According to *Joy et al.* [2006], this process is stochastic, in the sense that different structures decay at different speeds, and the observed large amplitude magnetic field dips correspond to inflated collapsing mirror structures.

[9] An alternative view of the large scale behavior of magnetosheath mirror modes was given by *Tátrallyay and Erdős* [2002]. The authors showed that if the change in mirror size is interpreted as a continuous growth as they are convected downstream through the magnetosheath, the measured growth rate is nearly an order of magnitude lower than the expected linear growth rate. They suggested that mirror modes might not always originate close to the bow shock and that the field line draping and temperature anisotropy increase close to the magnetopause may represent an important source of mirror instability [*Tátrallyay and Erdős*, 2005].

1.2. Theoretical Models

[10] The above experimental studies also show that the character of observed mirror modes depends on plasma β: low beta plasma ($\beta < 1$) is usually populated by dips, while peaks are mostly observed in high beta plasma ($\beta > 5$). The physics behind this correlation still remains largely a matter of speculation. *Kivelson and Southwood* [1996] proposed that while the linear growth rate should be identical for both types of mirror modes, different processes are responsible for the saturation of the instability resulting in different final states under different β. Several recent theoretical models based on various approximations were proposed to explain the difference between the physics of peaks and dips. Anisotropic fluid models with kinetic elements have been proposed by *Baumgärtel* [2001] and *Passot et al.* [2006]. Both of these models allow for nontrivial solutions corresponding to dips or peaks depending on the value of β and in both models the solution corresponding to dips remains stable even under plasma conditions that do not satisfy the threshold condition (1) and where linear theory predicts damping of mirror waves [*Borgogno et al.*, 2007]. This effect, previously identified in spacecraft data [*Bavassano-Cattaneo et al.*, 1998], is often referred to as bi-stability. Recently, *Kuznetsov et al.* [2007] proposed an alternative model based on perturbative expansion of Vlasov-Maxwell equations including the effects of finite ion Larmor radius. This theory also predicts that dips can exist deep in the mirror stable region, while peaks will be dissipated rapidly under such conditions. In addition, this model only allows magnetic peaks to be created by nonlinear saturation of mirror instability, while dips can be created by dynamic evolution of pre-existing large amplitude plasma perturbations. The above results on the relationship between mirror mode shape and plasma stability were also confirmed by hybrid simulations [*Baumgärtel et al.*, 2003] and numerical simulations based on the perturbative expansion of Vlasov-Maxwell equations (F. Califano et al., Nonlinear mirror mode dynamics: Simulations and modeling, submitted to *Journal of Geophysical Research*, 2007).

[11] Several recent works interpret the fully developed mirror modes as nonlinear self consistent Hall-MHD solutions of soliton type, independently of the instability responsible for their creation. *Baumgärtel* [1999] proposed such a soliton model of solar wind "magnetic holes" and showed that these solitons can exist under mirror stable plasma conditions both in the form of dips and peaks, but only magnetic dips are stable enough to survive for extended periods of time. *Stasiewicz* [2004] later extended the model to the case of anisotropic plasma and compared his model with Cluster observations of magnetosheath mirror modes. These models explain very well the observed properties of mirror modes in the final stage of development and the phenomenon of bi-stability, but do not consider their growth and relationship to the mirror instability, which limits their relevance to our study.

[12] In this article we present a statistical analysis of 2 months of Cluster observations of magnetosheath mirror modes together with a detailed case study of one dayside magnetosheath pass with an emphasis on mirror mode shape as a function of the location within magnetosheath, local plasma conditions, and sharp gradients in plasma parameters close to the magnetopause.

2. Data and Analysis Methods

[13] A large part of our study is based on a statistical investigation of properties of individual mirror structures and their correlation with the parameters of background plasma. In this section we describe the data analysis techniques used to create a database of mirror structures observed by Cluster during a period of 2 months.

2.1. Peakness and Properties of Individual Mirror Structures

[14] In order to investigate possible statistical relationships between the character of mirror modes, magnetosheath location and properties of the background plasma, one needs to develop a procedure to identify intervals of mirror mode activity and to calculate the properties of mirror structures in a short segment of satellite data. For the purpose of our study, we describe the mirror mode structures by two quantities: the depth of the corresponding depression of magnetic field from

the background value, or their height over the background in the case of magnetic field enhancements. The second quantity is so called "peakness" which identifies whether the mirror modes appear as peaks or dips.

[15] The peakness and mirror mode depth are calculated from magnetic field magnitude data provided by the FGM instrument of Cluster [*Balogh et al.*, 2001]. The high resolution data sampled at 22.5 Hz are first averaged to a sampling rate of 5 vectors per second and divided into nonoverlapping intervals of 5 minutes. The peakness and average mirror mode depth are then calculated for each subinterval from a continuous wavelet transform of the magnitude of the magnetic field intensity vector B using a Marr (or "Mexican hat") wavelet [*Mallat*, 1999] as a "mother wavelet". This particular wavelet function was chosen because of its close resemblance to the typical shape of mirror structures. The wavelet transform yields a real matrix of wavelet coefficients $W(t, s)$ that represents the content of structures similar to the mother wavelet rescaled to a given scale s and centered around time t. In this work, we normalize the scale s to be the equivalent Fourier wavelength of the Marr wavelet [*Meyers et al.*, 1993] defined as the wavelength corresponding to a maximum of the Fourier transform of the wavelet base function. This normalization is practical when interpreting the scale in terms of k-vectors and in the case of Marr wavelet it also roughly corresponds to the naive definition of mirror mode scale as the total width of magnetic field perturbation.

[16] These wavelet coefficients are next integrated over scales

$$b(t) = \int_{s_{\min}}^{s_{\max}} W(t,s)\frac{ds}{s^{3/2}}; \tag{3}$$

this new time series $b(t)$ represents the total wavelet content between scales $s_{\min}$ and $s_{\max}$ or in other words the original time series bandpass filtered using a wavelet filter. For the purpose of this study, the range of scales was set to $s_{\min} = 1$ s and $s_{\max} = 60$ s which corresponds to typical mirror mode time scales. The peakness $\mathcal{P}$, for a given interval, is then defined as the skewness of the time series $b(t)$:

$$\mathcal{P} = \frac{\left\langle \left(b(t) - \bar{b}\right)^3 \right\rangle}{\left\langle \left(b(t) - \bar{b}\right)^2 \right\rangle^{\frac{3}{2}}}. \tag{4}$$

Skewness of a distribution function gives a measure of the degree of its asymmetry [*Hahn and Shapiro*, 1994]. It is therefore possible to interpret $\mathcal{P}$ as a statistical quantity identifying whether the mirror modes have a character of peaks or dips: the distribution built from the time series $b(t)$ for the case of dips will possess a pronounced negative tail reflecting the contribution of strongly negative wavelet coefficients corresponding to the magnetic field depressions (and analogously for the case of peaks). Our tests of the method on a large number of intervals indicate that if several unambiguous mirror modes are contained within a studied interval, the sign of the peakness corresponds to their classification by visual inspection. In the ambiguous cases the value of $\mathcal{P}$ is usually close to zero. Two typical cases with corresponding values of peakness are shown in Figure 1.

[17] An alternative and simpler technique to identify the shape of mirror structures would be to calculate simple skewness of a digitally filtered time series. This approach has been recently used by V. Génot et al. (manuscript in preparation, 2007) in an independent mirror mode study. However, we chose our wavelet approach, because it properly respects the nonsinusoidal nonperiodic nature of mirror modes.

[18] Once the peakness is known, we proceed to identify the average depth of mirror structures in the given interval. For the case of negative peakness, we apply the following algorithm: The time series $b(t)$ is searched for local extreme points $t_{ext}^{(i)}$ and for each of these minima and maxima we identify a corresponding local extremum in the matrix of wavelet coefficients $W(t_i, s_i)$. For extremum $t_{ext}^{(i)}$, this is performed by searching the matrix for a maximum/minimum in an interval $t_{ext}^{(i-1)} < t < t_{ext}^{(i+1)}$.

[19] Local minima that are deeper than 20% of the global minimum ($b(t_{ext}^{(j)}) < 0.2 \min b(t)$ - note that $\min b(t) < 0$) are considered as candidates for mirror structures. For every such minimum, the corresponding wavelet scale s_j gives an estimate of the width of the mirror mode and the structure depth is calculated from the original magnetic field intensity as a difference of the background field and field at the minimum $d_j = |\frac{1}{2}(|B(t_{j-1})| + |B(t_{j+1})|) - |B(t_j)||$. If the scale of the structure s_j exceeds a threshold of 40 seconds, it is considered too wide for a mirror mode and it is removed from from the data set. The output of the automated analysis of each 5 minute snapshot are the following quantities: peakness $\mathcal{P}$, number of mirror structures within the snapshot N, and average structure depth $d = \frac{1}{N}\sum_{i=1}^{N} d_i$.

2.2. Cluster Magnetosheath Mirror Mode Database

[20] The database used to investigate the statistical properties of mirror modes was created by applying the procedure described in the previous section to 2 months of Cluster magnetosheath passes. We chose a period from November 15, 2005 to January 14, 2006 when Cluster was sampling the dusk sector of the magnetosheath and satellites were approximately 10,000 km apart. First, we restricted the data to intervals where satellites were most likely located in the magnetosheath and the local plasma conditions were favorable for creation of mirror modes. Data were considered to be acceptable magnetosheath data under the following conditions:

[21] 1. Spacecraft 3 was not further than 2 R_E from average model magnetopause [*Shue et al.*, 1997] in the earthward direction and less than 2 R_E from the average model bow shock [*Farris et al.*, 1991] in the outward direction.

[22] 2. CIS ion instrument [*Reme et al.*, 1997] was in magnetosheath mode.

[23] 3. $\beta_{\|} > 1$.

[24] 4. $|B| > 10$ nT.

[25] In the next step, we choose among the magnetosheath data all intervals that contain some mirror mode activity. This selection is based on the polarization properties of magnetic field fluctuations and on the results of the mirror mode identification technique described in section 2.1. The data that passed the above tests were next

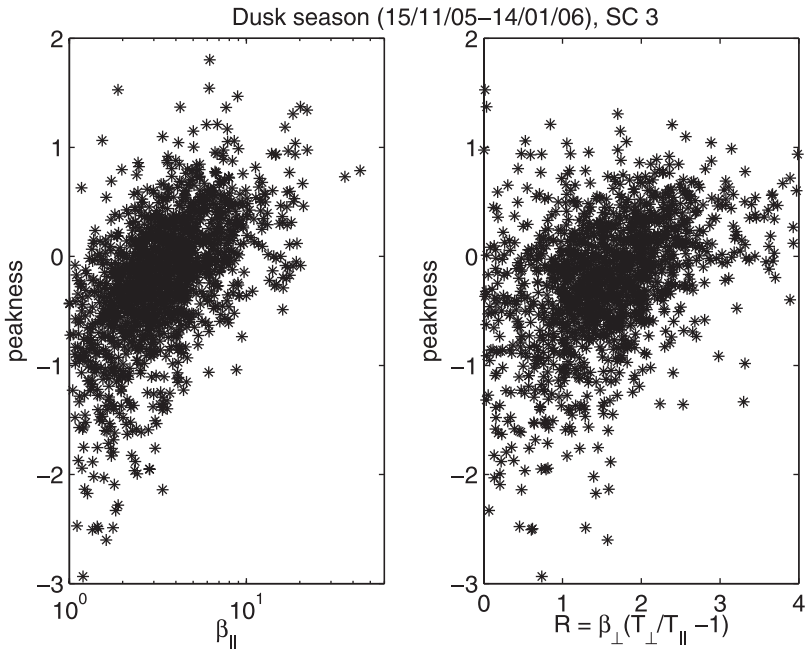

Figure 2. Dependence of peakness of mirror modes on parallel plasma beta and mirror instability parameter R.

divided into nonoverlapping 5 minute intervals and both the standard maximum variance analysis [*Sonnerup and Sheible*, 1998] and the above mirror mode analysis were applied to each of these subintervals. Because the mirror modes are, in an ideal case, linearly polarized with a maximum variance direction oriented at a small angle with respect to the background magnetic field we select only waveforms consistent with this property. A similar criterion was previously applied by *Tátrallyay and Erdős* [2005]. We therefore finally include the interval in the database of mirror mode events if the following conditions are met:

[26] 1. The ratio of the largest and intermediate eigenvalues of the variance matrix $\lambda_{\max}/\lambda_{int}$ is larger than 1.5.

[27] 2. The ratio of the two smallest eigenvalues of the variance matrix $\lambda_{\min}/\lambda_{int}$ is larger than 0.3.

[28] 3. The angle between the maximum variance direction and ambient magnetic field is smaller than 30°.

[29] 4. The wavelet technique identified at least 2 mirror structures within the interval.

[30] For the dusk season of 2005/2006, this procedure identified 1533 mirror mode intervals. For each of these intervals we further calculated the mirror mode properties (peakness and depth) for all four Cluster spacecraft. For spacecraft 1 and 3, where the HIA sensor of the CIS instrument was operational, we used the on-board calculated ion moments from this instrument to evaluate the average ion perpendicular and parallel temperature ($T_{\perp}$, $T_{||}$), density n and corresponding betas $\beta_{\perp,||} = 2\mu_0 nkT_{\perp,||}/|B|^2$. All statistical results presented later in this paper are based on this database of mirror mode and plasma parameters.

[31] The distribution of the scales of mirror structures was evaluated in order to check the influence of the 40 second maximum width required for inclusion of a mirror mode in the database. The scales of structures in our data set follow a bell shaped distribution with a mean value of 11.95 seconds where 98% of the values fall between 3.48 s and 23.85 s. The expected number of observed mirror modes, removed because of the 40 second width limit, can be therefore considered negligible. When these temporal scales are converted to spatial scales using plasma flow velocity and normalized to local proton Larmor radius ρ_L, we obtain a distribution with a mean scale of 39.1 ρ_L with 98% of values between 5 ρ_L and 85.4 ρ_l. Although the interpretation of the scales of mirror modes is beyond the scope of this paper, we use this result in section 7 to asses the importance of finite Larmor radius effects.

3. Correlation Between the Shape of Mirror Modes and Local Plasma Parameters

[32] As we already discussed in section 1, several previous experimental studies [*Joy et al.*, 2006; *Bavassano-Cattaneo et al.*, 1998] have shown that the shape of mirror structures is related to local plasma beta. Specifically, low beta conditions $\beta < 2$ are associated with observations of dips while peaks are usually observed in higher beta plasma.

[33] The expected relationship between peakness and plasma beta is easily identified in our mirror mode data set as shown in the left panel of Figure 2. Because magnetosheath plasma in the presence of mirror modes tends to follow the marginal stability path, where the instability growth rate is kept close to zero, it is natural to investigate how the character of mirror modes changes as plasma conditions change between a region of stability to an unstable state.

[34] To investigate this relationship, we introduce a parameter

$$R = \beta_{\perp}\left(T_{\perp}/T_{||} - 1\right) \tag{5}$$

which quantifies the deviation of plasma from stability given by the classical threshold condition (1). An unstable plasma state is thus represented by values of R greater than

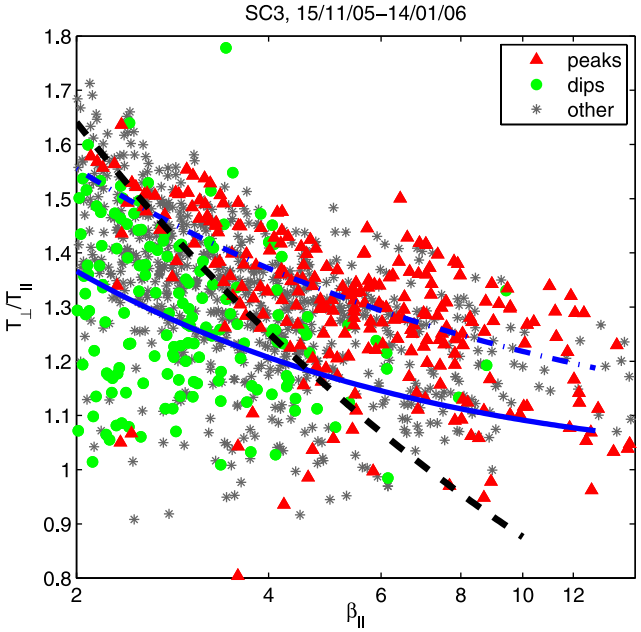

Figure 3. Distribution of mirror modes of different types in the anisotropy-beta plane. Red triangles denote peaks with $\mathcal{P} > 0.3$, green filled circles dips ($\mathcal{P} < -0.6$) and the remaining ambiguous mirror mode events are marked by grey stars. Solid blue line shows the theoretical mirror threshold (equation (1)), dash-dotted blue line the empirical marginal stability relation (2) with $a = 0.83$ and $b = 0.58$, and the black dashed line is the fitted boundary between peaks and dips (6).

one and the linear growth rate of the mirror instability is proportional to $R - 1$ [*Hasegawa*, 1969; *Southwood and Kivelson*, 1993].

[35] The right panel of Figure 2 shows that there is a clear relationship between the peakness and parameter R. When plasma is in an unstable state, peakness is predominantly positive and magnetic field enhancements (peaks) are observed, while smaller values of R are associated with magnetic field dips. Note that for stable conditions ($R < 1$), mirror modes are observed almost exclusively in the form of dips. The existence of mirror modes under stable conditions can be explained by the phenomenon of bi-stability [*Baumgärtel*, 2001] and our analysis experimentally proves that such mirror modes appear as magnetic dips, consistent with the theoretical and numerical results [*Kuznetsov et al.*, 2007; *Baumgärtel et al.*, 2003]. The above dependence of the character of mirror modes on instability parameter R has also been recently studied by V. Génot et al. (manuscript in preparation, 2007) in a simultaneous independent study with similar conclusions.

[36] The parameters R and $\beta_{||}$ are by definition mutually dependent and it is therefore difficult to decide on experimental basis which one of these determines the shape of mirror modes. Some insight into this problem can be gained from Figure 3. In this plot we show the distribution of mirror mode events in the anisotropy-beta plane marking the events with an above-threshold peakness ($\mathcal{P} > 0.3$) by red triangles and events with below-threshold peakness ($\mathcal{P} < -0.6$) by green filled circles. In total, our data set contains 287 peaks (18.7%), 609 dips (39.7%) and 637 ambiguous intervals (41.6%); these data are roughly consistent with the statistics of *Joy et al.* [2006] from the magnetosheath of Jupiter. For better clarity of the plot, we only included events where $\beta_{||} > 2$. The two thresholds were chosen based on the overall distribution of peakness in our data set to identify unambiguous peaks and dips. Ambiguous events are marked by black asterisks. The two superimposed curves correspond to the threshold condition (1) transformed to anisotropy-$\beta_{||}$ coordinates (solid line) and the empirical marginal stability relation derived by *Fuselier et al.* [1994] (dash-dotted line). In the figure we see a relatively clear boundary separating peak from dips, but this line does not correspond to either of the proposed relations. That boundary can be approximately fitted by a power law function in $\beta_{||}$ by finding a function that minimizes the number of peaks falling below its graph plus the number of dips above the line. This technique yields a relation

$$\frac{T_\perp}{T_{||}} = \frac{2.15}{\beta_{||}^{0.39}} \tag{6}$$

shown as the black dashed line Figure 3. This function gives a significantly better fit to the data than equation (2) with any combination of parameters a and b.

[37] Clearly, the shape of mirror modes is not completely determined by neither $\beta_{||}$ nor the parameter R alone, but the two types of mirror structures occupy distinct regions of the anisotropy-$\beta_{||}$ plane. The following conclusions can be drawn from Figure 3:

[38] 1. Dips are observed mostly for $\beta_{||} < 5$.

[39] 2. Peaks are usually observed above the threshold line $R > 1$, for a whole range of $\beta_{||}$ from 2 to 15.

[40] 3. Mirror modes observed in the stable region $R < 1$ are likely to have the form of magnetic dips. Unambiguous dips can be found relatively far from the threshold suggestive of the bi-stability phenomenon.

[41] These conclusions agree very well with the theoretical and numerical studies discussed above in section 1.2 where the authors show that magnetic dips (and dips only) can survive the transition of plasma to the stable state while peaks can only exist under unstable plasma conditions above the mirror threshold. According to this theory, dips can exist both above and below threshold which is also consistent with our analysis.

4. Case Study of Cluster Magnetosheath Crossing

[42] As shown by previous studies [*Bavassano-Cattaneo et al.*, 1998; *Joy et al.*, 2006], mirror modes change character as they are convected closer to the magnetopause and most importantly as they reach the plasma depletion layer (PDL) where plasma expands and its properties change sharply with distance from the magnetopause [*Anderson et al.*, 1994]. In this section, we examine one particular Cluster crossing of dayside magnetosheath with an emphasis on the spatial distribution of mirror mode shape and corresponding plasma parameters relative to the magnetopause.

[43] For this case study we chose a data set from March 1, 2006 when Cluster orbited in an approximately tetrahedral configuration with spacecraft separations ranging from 4000 km to over 10,000 km and the orbit ellipse was

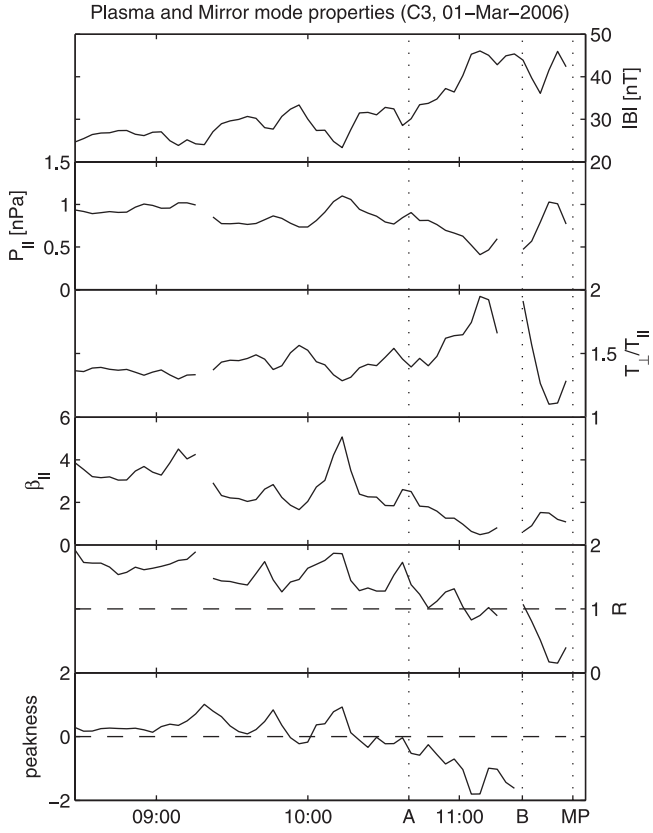

Figure 4. Plasma and mirror mode properties as observed by Cluster 3 during the magnetosheath pass on March 1, 2006. (top to bottom) Magnetic field magnitude, parallel ion pressure, ion temperature anisotropy, parallel ion β, mirror instability parameter R and peakness $\mathcal{P}$. Points A and B mark the approximate time of entry into the plasma depletion layer and time when mirror modes disappeared respectively. MP indicates the time of magnetopause crossing.

located approximately in the X-Z GSE plane. On that day Cluster 3 crossed the bow shock at approximately 6:58 UT and the magnetopause at 11:40. Cluster 4 followed a very similar orbit with a 1 hour delay crossing the bow shock at 8:19 and magnetopause at 12:45.

[44] Selected plasma parameters for this magnetosheath pass together with estimated peakness and mirror instability parameter R are shown in Figure 4. Point A on the horizontal axis marks the approximate time when satellite entered the PDL: magnetic field magnitude starts to increase with a decreasing distance to the magnetopause and the increased magnetic pressure is compensated by a decrease in plasma pressure, density and consequently plasma β. The effect of this plasma expansion on mirror instability is clearly seen in the two bottom panels. Outside of the PDL, the peakness is in general positive and Cluster observed mirror modes in the form of peaks. The instability parameter R is larger than one, indicating that plasma was in a mirror-unstable regime. As the spacecraft enters the plasma depletion layer, the sudden change in plasma properties leads to a sharp drop in R to values corresponding to mirror-stable plasma. The observed mirror structures reflect this fact by changing their character from peaks to dips. As Cluster reaches point B, the value of R starts dropping sharply and mirror modes disappear almost immediately.

[45] Figure 5 shows the same magnetosheath pass as a hodogram in the anisotropy-β plane. Different markers are used to indicate the character of mirror structures at a given time. The two superimposed lines represent the threshold condition (1) and a least-squares fit of (2) to the data from this pass. The fitted values of parameters were $a = 0.66$ and $b = 0.49$ which is reasonably consistent with the parameters obtained in previous studies [e.g., *Fuselier et al.*, 1994]. This figure conveys the information presented above in a clearer form: under varying plasma conditions, the mirror instability keeps the plasma in a marginally unstable state significantly above the (1) line. The rapid plasma expansion in the PDL then drives plasma towards a more stable state, where the hodogram closely follows the threshold (1) and character of mirror structures changes from peaks to dips. Here the plasma is stable or only very weakly unstable with respect to the mirror instability, yet we still observe mirror structures, but exclusively in the form of dips.

[46] The above results suggest that mirror mode properties change abruptly due to plasma expansion in the PDL and the magnetopause distance is likely an important determining factor of their shape. To test this conclusion, we investigated if mirror mode properties are consistent at the same magnetopause distance over time. We used data from Cluster spacecraft 3 and 4 which followed approximately the same trajectory through the magnetosheath with a separation of 10,000 km along the orbit which translates to approximately 1 hour delay of spacecraft 4 after spacecraft 3. Figure 6 shows the mirror mode peakness measured by these spacecraft as a function of time (top panel) and as a function of distance to the model magnetopause [*Shue et al.*, 1997] rescaled to match the observed magnetopause crossings (bottom panel).

[47] The bottom panel clearly shows that for this particular event, the dependence of peakness on the magnetopause distance is almost identical for both spacecraft. This suggests that the change of mirror mode regime from peaks to dips is a spatial effect driven by the change of plasma parameters in the vicinity of the magnetopause. From the figure we can further conclude that this transition occurs at a distance of approximately 2 R_E from the magnetopause.

[48] The above observations are fully consistent with magnetosheath mirror mode models of *Bavassano-Cattaneo et al.* [1998] and *Joy et al.* [2006] and provide further experimental insight into the dynamics of mirror structures. With respect to the conclusions of section 3 of this paper, we propose that the character (peakness) of mirror modes is largely determined by spatial variation of plasma parameters. Mirror structures created behind the bow shock are convected downstream to reach nonlinear saturation in the middle magnetosheath, in this case resulting in the formation of nonperiodic peaks. At this stage, plasma is kept in a marginally unstable state above the threshold (1). As the plasma flow reaches the PDL, it undergoes a rapid expansion forcing plasma into a mirror-stable state. Mirror structures survive this transition, but they assume the form of dips under such conditions. The theoretical framework of *Kuznetsov et al.* [2007], *Passot et al.* [2006], and *Baumgärtel* [2001] allows for an interpretation of this

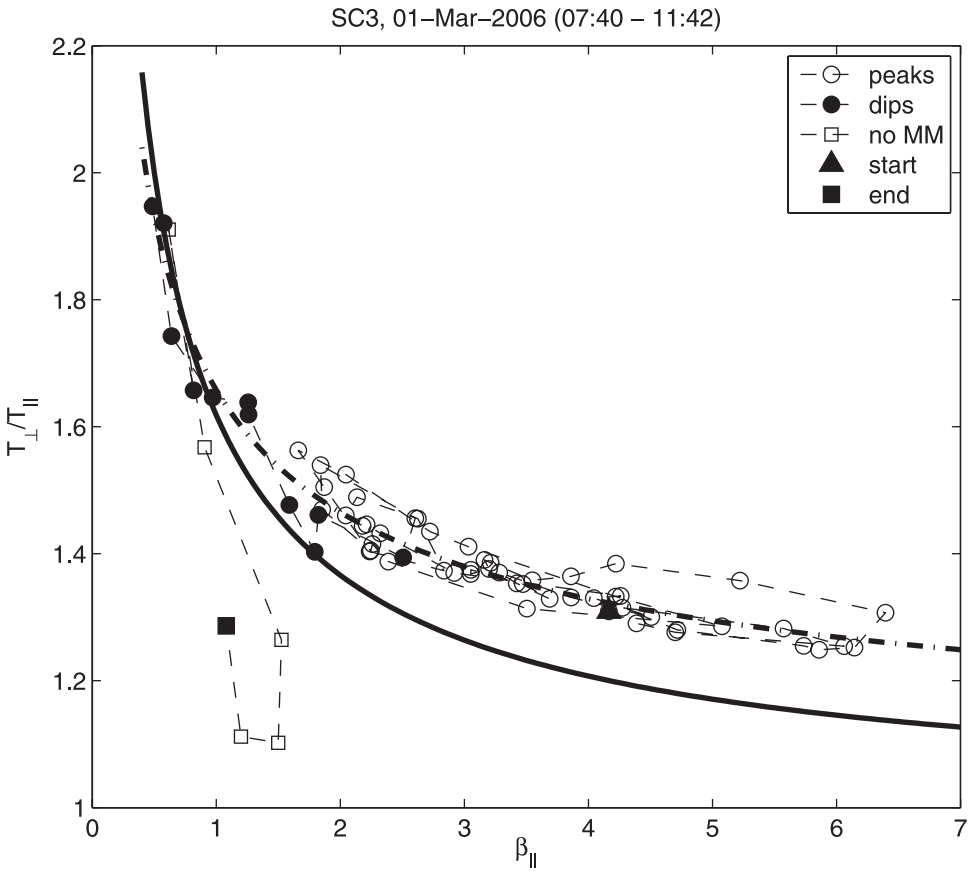

Figure 5. A hodogram of the evolution of temperature anisotropy and beta during the magnetosheath pass on March 1, 2006. Different markers along the path indicate the observed type of mirror modes. The superimposed solid line represents the theoretical mirror mode threshold given by equation (1) and the dashed line is a least squares fit of general "marginal stability" relation (equation (2)) to the data.

transition: mirror peaks in the magnetosheath typically appear as trains of multiple structures. While the peaks cannot exist under stable plasma conditions, such train of structures represents a large enough perturbation in magnetic field and plasma that can, under external forcing, evolve into a series of magnetic dips. A similar behavior has been observed in recent hybrid simulations such as those presented by *Trávníček et al.* [2007]. According to the authors (P. Hellinger, private communication, 2007; V. Génot et al., manuscript in preparation, 2007), the mirror structures in the expanding plasma box first appeared as peaks, but changed to dips as soon as the plasma reached a mirror-stable state.

5. Dependence of the Shape and Size of Mirror Structures on Magnetopause Distance

[49] In the above discussion, we have shown that mirror mode properties are largely determined by spatial inhomogeneities of plasma in the magnetosheath and their shape and size are strongly correlated with the distance to the magnetopause. In this section we use multipoint Cluster measurement to investigate this dependence in more detail. Simultaneous measurements from two spacecraft separated by over 10,000 km allow the spatial variation of mirror mode properties to be characterized at scales comparable with 1 Earth radius, completely eliminating the effect of temporal magnetosheath variations.

[50] Figure 7 shows how peakness and mirror mode depth normalized to background field levels vary as a function of distance to the magnetopause. The scatter plots were obtained from the mirror mode observations database described earlier by calculating the difference in the respective mirror mode parameters between two spacecraft (C2 and C4). This difference is always calculated as the value measured on the spacecraft further away from the magnetopause (GSE position $\vec{r}_1$) minus the value measured on the other satellite (GSE position $\vec{r}_2$). The difference is plotted against the projection of spacecraft separation onto the local model magnetopause normal denoted by $\Delta_{MP} = (\vec{r}_1 - \vec{r}_2) \cdot \vec{n}$, where $\vec{n}$ is a unit vector in the direction of magnetopause normal.

[51] Figure 7 shows the two most significant systematic trends revealed by the analysis. The right panel confirms the previously discussed observation that peaks are more often observed in the middle magnetosheath while mirror modes closer to the magnetopause are more likely to appear in the form of dips. This multispacecraft analysis extends this statement by giving an estimate of the the spatial scale of this transition. For $\Delta_{MP} > 1\ R_E$, the mean difference between peakness on the two spacecraft is 0.22 with the standard deviation of the mean estimate equal to 0.026. The

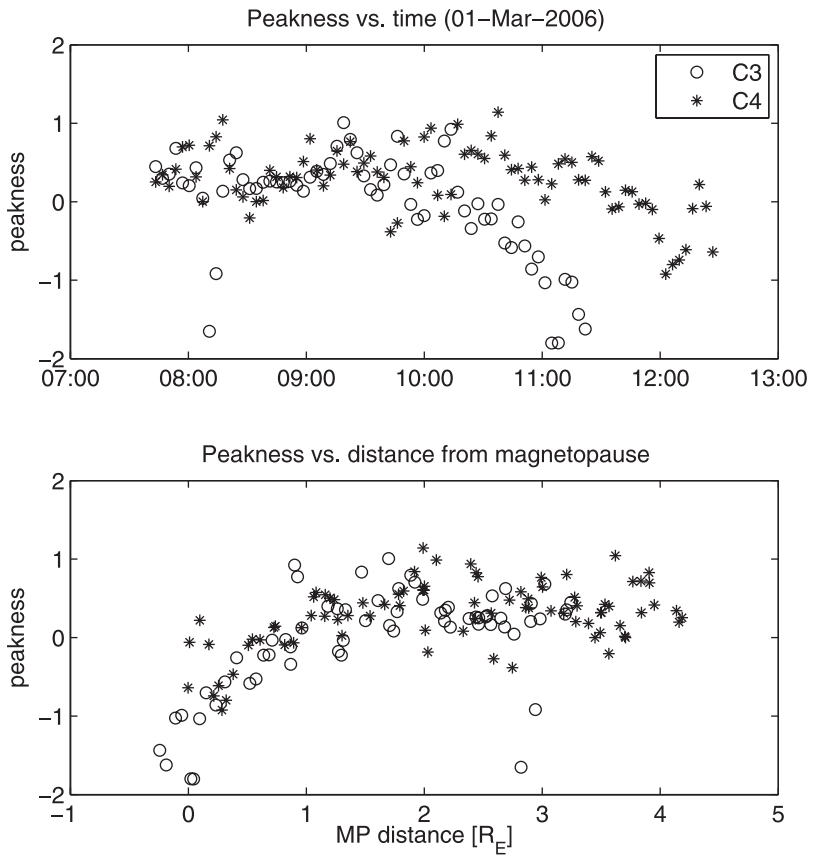

Figure 6. The dependence of peakness $\mathcal{P}$ on time (top) and on a distance from model magnetopause (bottom) for satellites 3 and 4 during the magnetosheath pass on March 1, 2006.

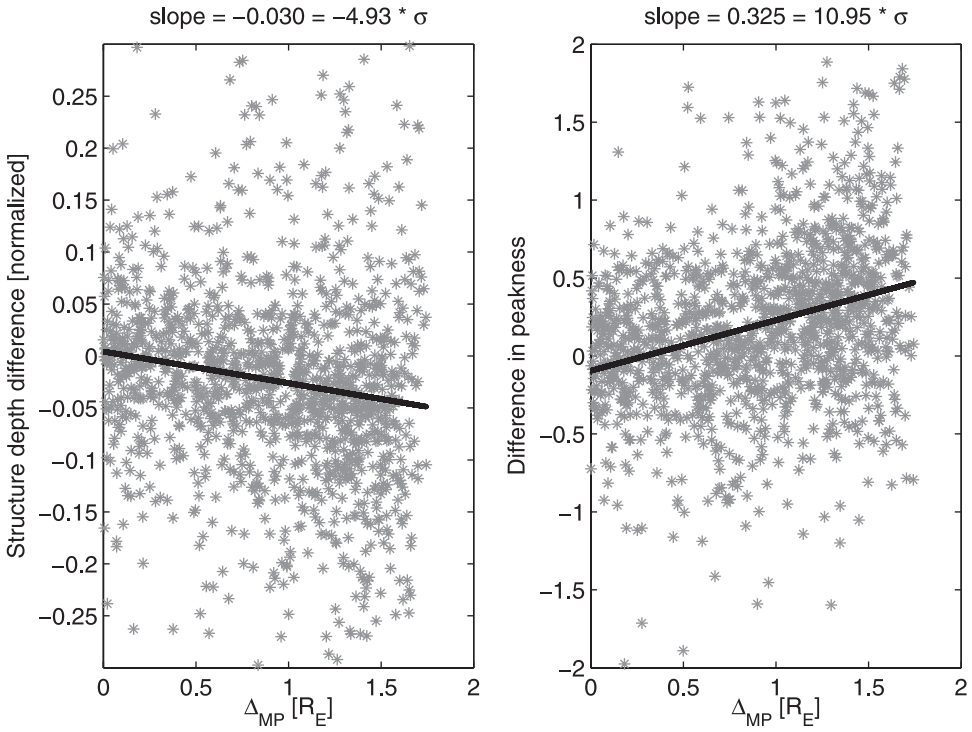

Figure 7. Difference in normalized mirror mode depth (left) and peakness (right) between two Cluster spacecraft (C2 and C4) as a function of the separation of the two spacecraft projected onto the local magnetopause normal Δ_{MP}. Solid lines indicate a trend obtained by linear regression analysis of the data.

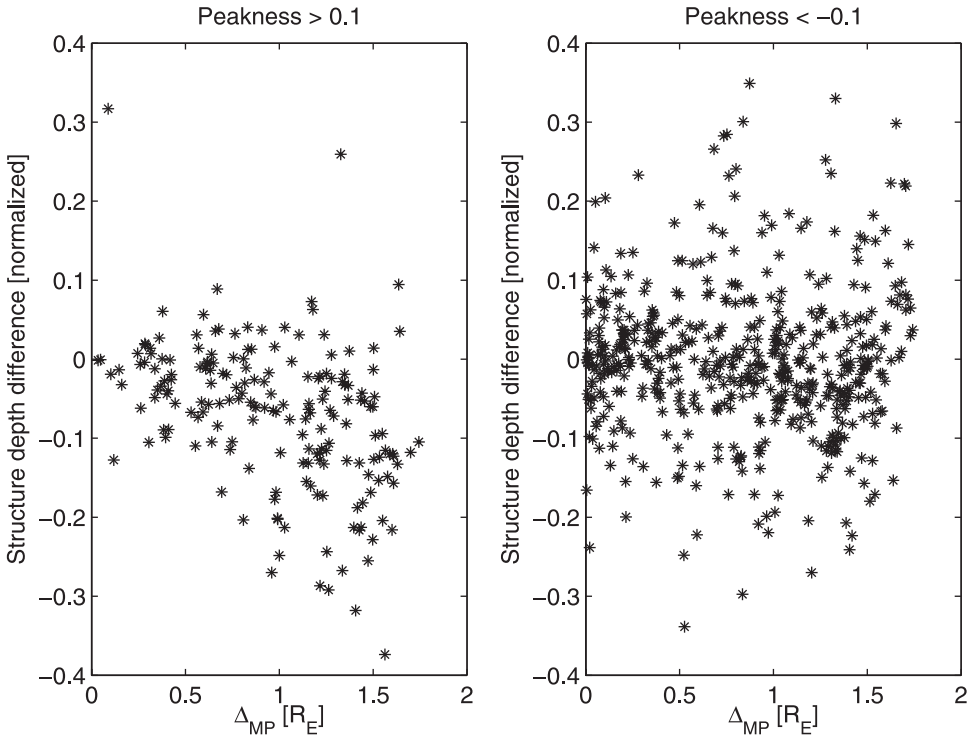

Figure 8. Difference in normalized mirror mode depth between two Cluster spacecraft (C2 and C4) as a function of spacecraft separation along the local magnetopause normal Δ_{MP}. (left) Values corresponding to all peaks in the data set ($\mathcal{P} > 0.1$). (right) The same dependence for dips ($\mathcal{P} < -0.1$).

difference in peakness is therefore already statistically significant at the distance of 1 R_E. Taking into account the linear trend in peakness 0.325 R_E^{-1}, we can safely conclude that the transition from peaks to dips typically occurs over spatial scales of 2–3 R_E.

[52] The left panel of Figure 7 shows the dependence of the difference in normalized depth of mirror structures for the same pair of spacecraft as a function of Δ_{MP}. The linear trend in the plot confirms that the depth of mirror structures increases with decreasing distance to the magnetopause. Figure 8 further disambiguates the effect by showing this dependence for peaks and dips separately. Left panel shows the dependence for the same data set, where only data points corresponding to observation of peaks (peakness > 0.1 on both spacecraft) were included and right panel shows the analogous analysis for magnetic dips (peakness < −0.1). Clearly, the decreasing trend in the data is entirely due to peaks: the left panel of Figure 8 shows that for peaks the difference in depth is mostly negative (meaning that the satellite closer to the magnetopause observes larger peaks) and increases in absolute value with Δ_{MP}. On the other hand, the right panel (dips) shows a symmetric distribution of positive and negative values and almost no dependence on Δ_{MP}. Linear regression analysis yields a trend of only $b = -0.18\ \sigma$, where σ is the standard deviation. The depth of dips therefore remains stable at spatial scales of 1–2 R_E, while peaks become significantly higher as they approach the magnetopause.

[53] While peaks are on average larger than dips (mean normalized mirror mode depth for the above data set evaluates to 0.392 ± 0.009 for peaks and 0.368 ± 0.005 for dips, where the errors are standard deviations of the estimates of the mean), their size varies significantly over the magnetosheath and increases as they are convected towards the magnetopause. Since peaks are observed predominantly in the middle magnetosheath, more than 2 R_E away from the magnetopause, this observation is consistent with the models of *Bavassano-Cattaneo et al.* [1998] and *Joy et al.* [2006] and probably corresponds to growth and steepening of mirror modes as they approach the nonlinear saturation state. The theoretical model of *Kuznetsov et al.* [2007], which only allows peaks to be created by nonlinear evolution of mirror instability, is also consistent with this conclusion.

6. Mirror Instability in the Magnetosheath Flanks

[54] In this section we discuss how mirror mode properties evolve as the plasma is convected further downstream towards the magnetosheath flanks. Magnetosheath plasma flow lines originating far from subsolar point approach the magnetopause very slowly and may not reach the proximity of magnetopause responsible for the processes discussed in the previous section. In the downstream magnetosheath flank region ($X_{GSE} <\sim 2\ R_E$), we can therefore expect significantly different patterns of mirror mode evolution.

[55] For this analysis we used the same statistical data set as previously (Dusk region, Nov 15, 2005 to Jan 14, 2006) but with several restrictions. Since Cluster orbit does not offer a very good coverage of the flank region, our statistical analysis is restricted by a downstream limit of $X_{GSE} > -4\ R_E$ below which the magnetosheath coverage is minimal. Since the magnetopause distance is significantly correlated with

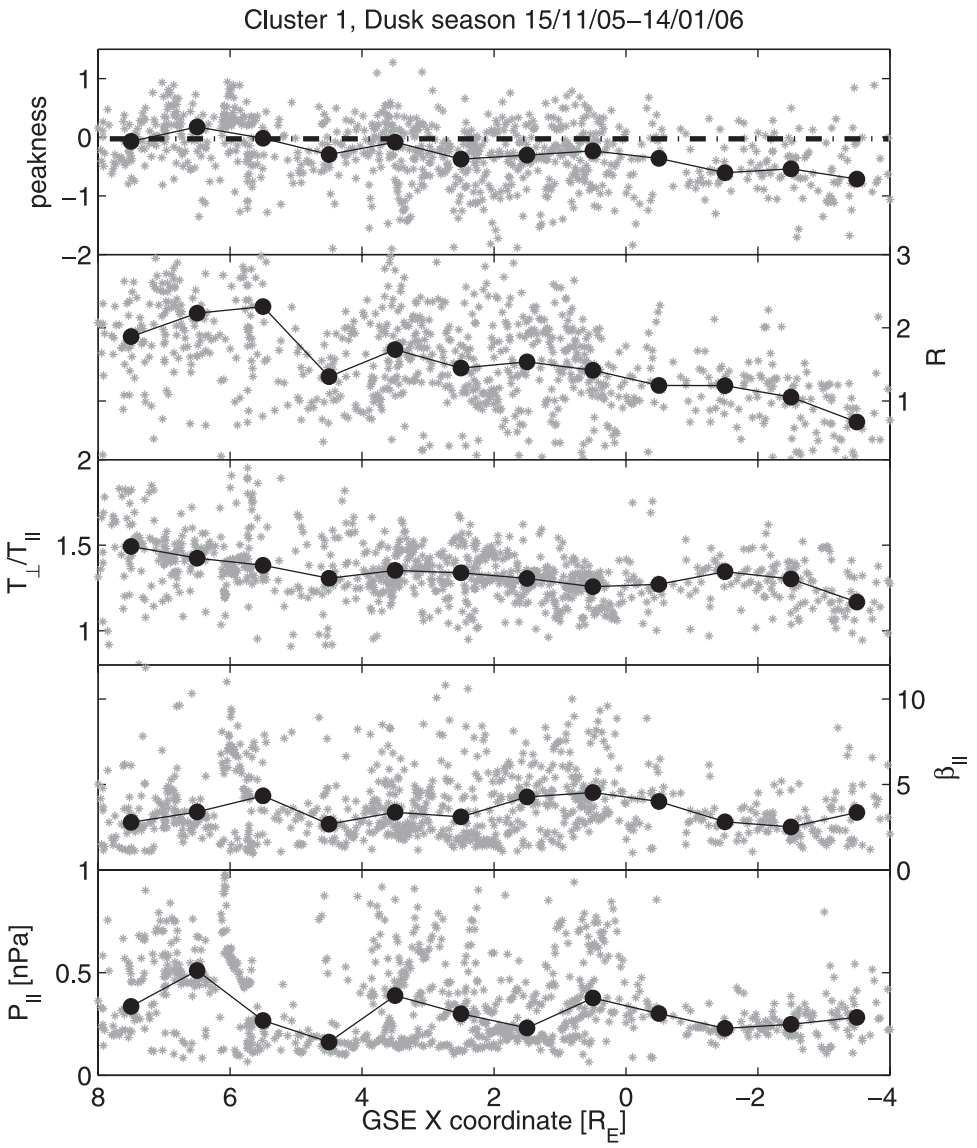

Figure 9. Plasma and mirror mode properties observed by Cluster 1 during dusk season 2005/2006 as a function of GSE X coordinate. (top to bottom) Peakness $\mathcal{P}$, mirror instability parameter R, ion temperature anisotropy, parallel ion β and parallel ion pressure. The black connected dots represent median values calculated for 1 R_E bins.

mirror mode properties, we further restricted our data set to include only observations performed when the distance of the spacecraft from the model magnetopause was between 1 and 4 R_E.

[56] Figure 9 shows selected plasma and mirror mode parameters for the above data set as a function of GSE X coordinate. Medians of the respective values calculated for 1 R_E bins were superimposed over the scatter plots to allow for better identification of trends. In the figure we see a definite decreasing trend in peakness (from an average value close to zero towards strongly negative values), R parameter (from strongly unstable plasma to mirror stable conditions) and temperature anisotropy. Linear regression for the above parameters yields the values of linear coefficients (normalized to their standard deviation) of $b = -12.25\ \sigma$ for peakness, $b = -14.29\ \sigma$ for R, and $b = -13.24\ \sigma$ for temperature anisotropy. On the other hand, no clear trend in $\beta_{\|}$ ($b = -1.06\ \sigma$) and only a weak trend in plasma pressure ($b = -4.53\ \sigma$) can be identified.

[57] This shows an example of behavior where the mirror mode peakness is clearly correlated with R but not with $\beta_{\|}$. The parallel pressure data indicates that magnetosheath plasma does not on average undergo significant expansion as it flows toward the downstream flanks (at least not in the near magnetosheath flanks $X_{GSE} > -4\ R_E$). Apparently, the decreasing temperature anisotropy is the cause of the decrease in mirror instability parameter R in this case and is most likely responsible for the change of mirror mode properties from mixed peak/dips situation ($\mathcal{P} \sim 0$) in the dayside magnetosheath to predominantly dips in the flanks.

[58] The above analysis confirms that mirror modes situated deeper in the flanks typically appear in the forms of dips. This effect has been previously noted by *Joy et al.* [2006] in Jupiter data, but their study could not resolve the

relationship of the mirror mode properties to local plasma conditions. The decrease in temperature anisotropy correlated with the decrease in mirror mode peakness can be interpreted in two ways: First, the lower values of anisotropy in the flanks can be a consequence of different shock conditions. The flow lines downstream in the magnetosheath are connected to bow-shock locations far from the subsolar point, which in general correspond to a weaker shock resulting in lower values of anisotropy. Alternatively, the lower anisotropy values can be caused by the action of the mirror and ion-cyclotron instabilities themselves as the convection time from the bow-shock is already long enough to allow the instabilities to decrease the original temperature anisotropy.

[59] In either case, this observation further supports our previous observation that mirror mode shape is related to plasma stability and that mirror structures under stable or near stable plasma conditions appear exclusively as dips. It complements the analysis presented in section 3 of this article by demonstrating a scenario, where the average change in the parameter R is not associated with a significant change in plasma β.

7. Summary and Discussion

[60] In this article, we presented a thorough analysis of magnetosheath mirror modes observed by Cluster, both from the statistical point of view and through a detailed case study, exploiting the multipoint nature of the Cluster data set. We investigated the correlation of peakness with both local β and parameter R related to the degree of instability of plasma. Since both these parameters are by definition (5) interdependent, a significant correlation is present in both cases. While the dependence on β has been noted in previous studies [*Bavassano-Cattaneo et al.*, 1998; *Joy et al.*, 2006], the dependence on R has not been assessed by previous experimental studies with the exception of a recent work of V. Génot et al. (manuscript in preparation, 2007). Our analysis shows that only magnetic dips appear in the mirror-stable region, while peaks are mostly observed when the plasma satisfies the mirror instability condition (1). This observation is in a very good agreement with recent theoretical models of *Kuznetsov et al.* [2007], *Baumgärtel* [2001], and *Passot et al.* [2006], numerical simulations based on the perturbative expansion of Vlasov-Maxwell equations (Califano et al., submitted manuscript, 2007), and hybrid simulations [*Baumgärtel et al.*, 2003; *Trávníček et al.*, 2007; P. Hellinger, private communication, 2007]. In these studies the authors show that only magnetic peaks can be created as a nonlinear stage of mirror instability and they can only exist under unstable plasma conditions ($R > 1$). On the other hand, dips represent stable solutions even deep inside the stable region and can be created from large amplitude initial perturbations.

[61] We provide further experimental evidence for the significance of parameter R by investigating the dependence of mirror mode properties and plasma parameters in the magnetosheath flanks on their location within the magnetosheath measured using the GSE X coordinate. This analysis shows an example scenario, where a change in peakness is clearly correlated with a trend in R, but no associated significant trend in plasma β is observed.

[62] Using a multipoint case study of one magnetosheath pass it was demonstrated that mirror mode properties are strongly correlated with magnetopause distance. Plasma in the middle magnetosheath is mostly populated by peaks and follows a marginal stability path well above the instability threshold. A sudden change in mirror mode properties occurs at a distance of approximately 2 R_E from the magnetopause, where peaks turn into dips and plasma parameters switch to a different path in the anisotropy-β space, very close to a mirror stable state. This change is probably related to rapid plasma expansion in the plasma depletion layer.

[63] Multipoint statistical analysis was then used to show that such change in the character of mirror modes is a statistically significant phenomenon in the magnetosheath and that the height of peaks increases as they approach this turning point. The depth of dips, on the other hand, is not related to their distance to the magnetopause, which supports the hypothesis of their different dynamic properties.

[64] Finally, based on the above results, we propose an extension to the model of spatial distribution and evolution of mirror structures in the magnetosheath formulated previously by *Bavassano-Cattaneo et al.* [1998] and *Joy et al.* [2006]. In accordance with their model, mirror modes are created behind the bow shock as quasi-sinusoidal waves. As they are convected through the magnetosheath, they continue to grow, assume the form of nonperiodic peaks due to their nonlinear evolution and eventually reach nonlinear saturation [*Kivelson and Southwood*, 1996]. Dips can also be observed in this region, either as a final stage of mirror instability or as stable structures created by evolution of trains of peaks under a change of plasma conditions. As the plasma reaches the proximity of magnetopause (approximately 2 R_E) it undergoes an expansion and is driven to a mirror stable state by a decrease in β and consequently in R. During this expansion, when R becomes sufficiently low, peaks become heavily damped and dips represent the only stable form of mirror-like structures that can be created from large amplitude perturbations of magnetic field. The dips eventually disappear very close to the magnetopause, where plasma deviates far from the instability threshold and becomes perturbed by the proximity of the magnetopause boundary.

[65] Further downstream in the magnetosheath flanks we observe mostly magnetic dips even at larger magnetopause distance, due to a gradual decrease in temperature anisotropy. As discussed in previous section, this decrease in anisotropy can be interpreted either by the action of mirror (and possibly other) instabilities that thermalize the plasma on its path from the bow shock toward the flanks or by the fact that plasma flow lines in the flanks typically originate at bow shock positions further away from the subsolar point, where the shock is weaker.

[66] The problem of finite Larmor radius effects (FLR) in the linear theory of mirror instability has recently been a subject of debate with the publication of a number of studies. *Pokhotelov et al.* [2004] revisited the linear kinetic theory of mirror instability and proposed that the threshold condition (1) is significantly modified by FLR effects, assuming that maximum mirror growth rate is attained at short wavelengths $k_\perp \rho_L \approx 1$, where $k_\perp$ is a perpendicular component of mirror mode wavevector. In a recent study, *Qu et al.* [2007] derived a dispersion relation of mirror modes using gyrokinetic theory and verified their analytical

results by comparison with gyrokinetic particle simulations. Their results confirm that the effect of the FLR on the instability threshold is important at small $k_\perp$ and that the mirror instability could generate waves at sufficiently small wavelengths $k_\perp \rho_L \approx 1$.

[67] The above results were later disputed by *Hellinger* [2007], who calculated the exact k-vector corresponding to the maximum growth rate from Vlasov-Maxwell kinetic theory. In the framework of this theory, the instability threshold is not modified by FLR effects, in accordance with the original work of *Hasegawa* [1969], and for near threshold mirror instability, the maximum growth rate is obtained at $k_\perp \rho_L \ll 1$. While the evolved mirror mode peaks and dips considered in our study are in general not in the regime of linear growth, the observed scales may still represent a reasonable approximation of the original wavelength. Using the mirror scale statistics presented at the end of section 2, we obtain an average value of $\langle |k|\rho_L \rangle = 0.19$ with 98% of observed values of $|k|\rho_L$ falling between 0.074 and 0.54. These values contradict the assumption of *Pokhotelov et al.* [2004], are roughly consistent with the results of *Hellinger* [2007] and justify our use of stability condition (1).

[68] The experimental study presented in this paper can be further improved especially with respect to the particle observations. Here we only used temperatures derived from the on-board calculated moments provided by the HIA sensor of the CIS instrument [*Reme et al.*, 1997]. The full distribution functions could be used to obtain more precise estimates of the temperature anisotropy together with some indication of the associated errors. A second experimental limitation of our study was the unavailability of alpha particle density and temperature measurements in magnetosheath plasma. It is well known that the Helium component of the plasma may significantly influence the threshold of mirror instability [*Gary et al.*, 1993; *Hellinger and Trávníček*, 2005]. The HIA sensor used in our study does not distinguish between the two species of ions and measures ''average'' temperature and density, where contributions of both species are added together. The other CIS sensor which measures the ion composition of plasma (CODIF) could be possibly used to separate the contribution of protons and alpha particles to density and temperature, but due to the sophisticated analysis involved, this is probably not plausible on a large volume of data required for the statistics. A future possible continuation of the study would involve an investigation of the spatial scales of individual mirror modes and their relationship to other plasma properties. A more detailed quantitative comparison with recent theory and numerical simulations is also required to improve our understanding of the problem.

[69] **Acknowledgments.** This work was performed in the framework of ISSI team ''The effect of ULF turbulence and flow chaotisation on plasma energy and mass transfer at the magnetopause''. Cluster work at Imperial College London is funded by STFC. E. Lucek is supported by a PPARC Fellowship. We also thank P. Hellinger and S. Schwartz for useful discussions.

[70] Zuyin Pu thanks the reviewers for their assistance in evaluating this paper.

References

Anderson, B. J., S. A. Fuselier, S. P. Gary, and R. E. Denton (1994), Magnetic spectral signatures in the Earth's magnetosheath and plasma depletion layer, *J. Geophys. Res.*, *99*, 5877–5891.

Balogh, A., et al. (2001), The Cluster Magnetic Field Investigation: overview of in-flight performance and initial results, *Ann. Geophys.*, *19*, 1207–1217.

Baumgärtel, K. (1999), Soliton approach to magnetic holes, *J. Geophys. Res.*, *104*, 28,295–28,308.

Baumgärtel, K. (2001), Fluid approach to mirror mode structures, *Planet. Space Sci.*, *49*, 1239–1247.

Baumgärtel, K., K. Sauer, and E. Dubinin (2003), Towards understanding magnetic holes: Hybrid simulations, *Geophys. Res. Lett.*, *30*(14), 1761, doi:10.1029/2003GL017373.

Bavassano-Cattaneo, M. B., C. Basile, G. Moreno, and J. D. Richardson (1998), Evolution of mirror structures in the magnetosheath of saturn from the bow shock to the magnetopause, *J. Geophys. Res.*, *103*, 11,961–11,972.

Borgogno, D., T. Passot, and P. L. Sulem (2007), Magnetic holes in plasmas close to the mirror instability, *Nonlin. Proc. Geophys.*, *14*, 373–383.

Burlaga, L. F., N. F. Ness, and M. H. Acuna (2006), Trains of magnetic holes and magnetic humps in the heliosheath, *Geophys. Res. Lett.*, *33*, L21106, doi:10.1029/2006GL027276.

Constantinescu, O. D., K.-H. Glassmeier, R. Treumann, and K.-H. Fornaçon (2003), Magnetic mirror structures observed by Cluster in the magnetosheath, *Geophys. Res. Lett.*, *30*(15), 1802, doi:10.1029/2003GL017313.

Erdős, G., and A. Balogh (1996), Statistical properties of mirror mode structures observed by Ulysses in the magnetosheath of Jupiter, *J. Geophys. Res.*, *101*, 1–12.

Farris, M. H., S. M. Petrinec, and C. T. Russell (1991), The thickness of the magnetosheath - Constraints on the polytropic index, *Geophys. Res. Lett.*, *18*, 1821–1824.

Fuselier, S. A., B. J. Anderson, S. P. Gary, and R. E. Denton (1994), Inverse correlations between the ion temperature anisotropy and plasma beta in the Earth's quasi-parallel magnetosheath, *J. Geophys. Res.*, *99*, 14,931–14,936.

Gary, S. P. (1992), The mirror and ion cyclotron anisotropy instabilities, *J. Geophys. Res.*, *97*, 8519–8529.

Gary, S. P., S. A. Fuselier, and B. J. Anderson (1993), Ion anisotropy instabilities in the magnetosheath, *J. Geophys. Res.*, *98*, 1481–1488.

Gary, S. P., M. E. McKean, D. Winske, B. J. Anderson, R. E. Denton, and S. A. Fuselier (1994), The proton cyclotron instability and the anisotropy/B inverse correlation, *J. Geophys. Res.*, *99*, 5903–5914.

Gary, S. P., B. Lavraud, M. F. Thomsen, B. Lefebvre, and S. J. Schwartz (2005), Electron anisotropy constraint in the magnetosheath: Cluster observations, *Geophys. Res. Lett.*, *32*, L13109, doi:10.1029/2005GL023234.

Génot, V., S. J. Schwartz, C. Mazelle, M. Balikhin, M. Dunlop, and T. M. Bauer (2001), Kinetic study of the mirror mode, *J. Geophys. Res.*, *106*, 21,611–21,622.

Hahn, G. J., and S. S. Shapiro (1994), *Statistical Models in Engineering*, John Wiley, New York.

Hasegawa, A. (1969), Drift mirror instability in the magnetosphere, *Phys. Fluids*, *12*, 2642–2650.

Hellinger, P. (2007), Comment on the linear mirror instability near the threshold, *Phys. Plasmas*, *14*, 082105.

Hellinger, P., and P. Trávníček (2005), Magnetosheath compression: Role of characteristic compression time, alpha particle abundance, and alpha/proton relative velocity, *J. Geophys. Res.*, *110*, A04210, doi:10.1029/2004JA010687.

Hellinger, P., P. Trávníček, A. Mangeney, and R. Grappin (2003), Hybrid simulations of the magnetosheath compression: Marginal stability path, *Geophys. Res. Lett.*, *30*(18), 1959, doi:10.1029/2003GL017855.

Horbury, T. S., E. A. Lucek, A. Balogh, I. Dandouras, and H. Rème (2004), Motion and orientation of magnetic field dips and peaks in the terrestrial magnetosheath, *J. Geophys. Res.*, *109*, A09209, doi:10.1029/2003JA010237.

Joy, S. P., M. G. Kivelson, R. J. Walker, K. K. Khurana, C. T. Russell, and W. R. Paterson (2006), Mirror mode structures in the jovian magnetosheath, *J. Geophys. Res.*, *111*, A12212, doi:10.1029/2006JA011985.

Kaufmann, R. L., J.-T. Horng, and A. Wolfe (1970), Large-amplitude hydromagnetic waves in the inner magnetosheath, *J. Geophys. Res.*, *75*, 4666–4676.

Kivelson, M. G., and D. J. Southwood (1996), Mirror instability II: The mechanism of nonlinear saturation, *J. Geophys. Res.*, *101*, 17,365–17,372.

Kuznetsov, E. A., T. Passot, and P. L. Sulem (2007), Dynamical Model for Nonlinear Mirror Modes near Threshold, *Phys. Rev. Lett.*, *98*(23), 235003.

Lucek, E. A., et al. (1999), Mirror mode structures observed in the dawn-side magnetosheath by Equator-S, *Geophys. Res. Lett.*, *26*, 2159–2162.

Mallat, S. (1999), *Wavelet Tour of Signal Processing*, Academic, New York.

McKean, M. E., D. Winske, and S. P. Gary (1994), Two-dimensional simulations of ion anisotropy instabilities in the magnetosheath, *J. Geophys. Res.*, *99*, 11,141–11,154.

Meyers, S. D., B. G. Kelly, and J. J. O'Brien (1993), An introduction to wavelet analysis in oceanography and meteorology: With application to the dispersion of Yanai waves, *Mon. Weather Rev.*, *121*, 2858–2866.

Pantellini, F. G. E., and S. J. Schwartz (1995), Electron temperature effects in the linear proton mirror instability, *J. Geophys. Res.*, *100*, 3539–3549.

Passot, T., V. Ruban, and P. L. Sulem (2006), Fluid description of trains of stationary mirror structures in a magnetized plasma, *Phys. Plasmas*, *13*, 102310, doi:10.1063/1.2356485.

Pokhotelov, O. A., R. Z. Sagdeev, M. A. Balikhin, and R. A. Treumann (2004), Mirror instability at finite ion-Larmor radius wavelengths, *J. Geophys. Res.*, *109*, A09213, doi:10.1029/2004JA010568.

Qu, H., Z. Lin, and L. Chen (2007), Gyrokinetic theory and simulation of mirror instability, *Phys. Plasmas*, *14*, 042108, doi:10.1063/1.2721074.

Reme, H., J. M. Bosqued, J. A. Sauvaud, et al. (1997), The Cluster Ion Spectrometry (CIS) Experiment, *Space Sci. Rev.*, *79*, 303–350.

Samsonov, A. A., M. I. Pudovkin, S. P. Gary, and D. Hubert (2001), Anisotropic MHD model of the dayside magnetosheath downstream of the oblique bow shock, *J. Geophys. Res.*, *106*, 21,689–21,700.

Schwartz, S. J., D. Burgess, and J. J. Moses (1996), Low-frequency waves in the Earth's magnetosheath: Present status, *Ann. Geophys.*, *14*, 1134–1150.

Shue, J.-H., J. K. Chao, H. C. Fu, C. T. Russell, P. Song, K. K. Khurana, and H. J. Singer (1997), A new functional form to study the solar wind control of the magnetopause size and shape, *J. Geophys. Res.*, *102*, 9497–9512.

Sonnerup, B. U. O., and M. Sheible (1998), Minimum and maximum variance analysis, in *Analysis Methods for Multi-Spacecraft Data*, edited by G. Paschmann and P. W. Daly, pp. 185–220, Int. Space Sci. Inst., Bern, Switzerland, and Eur. Space Agency, Paris, France.

Southwood, D. J., and M. G. Kivelson (1993), Mirror instability. I - Physical mechanism of linear instability, *J. Geophys. Res.*, *98*, 9181–9187.

Stasiewicz, K. (2004), Reinterpretation of mirror modes as trains of slow magnetosonic solitons, *Geophys. Res. Lett.*, *31*, L21804, doi:10.1029/2004GL021282.

Stix, T. H. (1962), *The Theory of Plasma Waves*, McGraw-Hill, New York.

Tátrallyay, M., and G. Erdős (2002), The evolution of mirror mode fluctuations in the terrestrial magnetosheath, *Planet. Space Sci.*, *50*, 593–599.

Tátrallyay, M., and G. Erdős (2005), Statistical investigation of mirror type magnetic field depressions observed by ISEE-1, *Planet. Space Sci.*, *53*, 33–40, doi:10.1016/j.pss.2004.09.026.

Trávníček, P., P. Hellinger, M. G. G. T. Taylor, C. P. Escoubet, I. Dandouras, and E. A. Lucek (2007), Magnetosheath plasma expansion: Hybrid simulations, *Geophys. Res. Lett.*, *34*, L15104, doi:10.1029/2007GL029728.

Tsurutani, B. T., et al. (1982), Lion roars and nonoscillatory drift mirror waves in the magnetosheath, *J. Geophys. Res.*, *87*, 6060–6072.

Walker, S. N., M. A. Balikhin, and M. Dunlop (2002), Mirror structures in the magnetosheath: 3D structures on plane waves, *Adv. Space Res.*, *30*, 2745–2750.

I. Dandouras, CESR-CNRS, Cedex 4 F-31028 Toulouse, France.

E. Lucek, Space and Atmospheric Physics Group, Blackett Laboratory, Imperial College, London SW7 2AZ, UK. (e.lucek@imperial.ac.uk)

J. Soucek, Department of Space Physics, Institute of Atmospheric Physics, Academy of Sciences of the Czech Republic, Bocni II/1401, Praha 4, 14131, Czech Republic. (soucek@ufa.cas.cz)